Semi-Blind Separation of Multiple Asynchronous Wideband Frequency Hopping Signals Based on MWC and Spectral Entropy Method

Mohsen Rezaee[1], Morteza Babaei [2], Mohammadreza Motedayen [3]
1- ICT Research Institute, Tehran, Iran.
Email: m.rezaeekh@itrc.ac.ir (Corresponding Author)
2- Imam Hossein Comprehensive University, Tehran, Iran.
Email: mbabaei @ihu.ac.ir
3- Faculty of Electrical Engineering Department, Imam Hossein University, Tehran, Iran.
Email: p9519894887@ ihu.ac.ir

ABSTRACT:
Wideband Frequency Hopping Spread Spectrum (FHSS) communications are widely used in both military and commercial applications. In military applications, it is very important to investigate these communications, especially when frequency hopping signals are received simultaneously by a single antenna. This paper investigates the problem of estimating interfering wideband asynchronous frequency hopping (FH) signals parameters with the same hop rate, and using narrow-band receivers. Due to minimal knowledge about the transmitted signals, the problem is analyzed in semi-blind mode. For this purpose, time-frequency (TF) processing has been applied to the modulated wideband converter (MWC) output. The proposed method consists of two stages; In the first stage, frequency-hopping signals with different amplitudes are received by a single antenna. By passing through baseband receivers, the TF distribution of the converter's output signal is obtained. In the next stage, by computing instantaneous spectral entropy (SE), and finding the local maxima in the spectrum, the hop time of each signal is obtained. We use MWC for sub-Nyquist sampling and simultaneous extraction of time and frequency information from signals while eliminating irrelevant signals. The results obtained from estimating hop time parameters demonstrate improved performance compared to other traditional source separation methods such as sparse linear regression (SLR). Based on evaluation metrics such as root mean squared error (RMSE), in lower signal-to-noise ratio (SNR) values, the amount of error has been substantially reduced.

KEYWORDS: Semi-Blind Separation, Modulated Wideband Converter, Time-Frequency Distribution, Spectral Entropy, Wideband Frequency-Hopping Signal.

1. INTRODUCTION

In recent years, spread spectrum telecommunications has been expanded due to its appropriate performance in different applications [1]. In the meantime, Frequency Hopping (FH) communication is one of the most essential types of spread spectrum communications in which the signal is controlled by a pseudo-random sequence and is spread across the entire spectrum [2].

Frequency-hopping communication is widely used in military and civilian communications due to its low probability of detection (and intercept) [3-5], high reliability, anti-jamming capability, and low sensitivity. Considering these features, estimating the parameters of FH signals is difficult, especially when there exist multiple interfering signals with no prior information about hop patterns [6-7]. In practical communications, the electromagnetic environment is very

Paper type: Research paper
https://doi.org/10.30486/MJTD.2024.901781
Received: 2 November 2023; revised: 18 March 2024; accepted: 29 April 2024; published: 1 June 2024
How to cite this paper: M. Rezaee, M. Babaei, M. R. Motedayen, **"Semi-Blind Separation of Multiple Asynchronous Wideband Frequency Hopping Signals Based on MWC and Spectral Entropy Method"**, *Majlesi Journal of Telecommunication Devices*, Vol. 13, No. 2, pp. 97-111, 2024.

complex, especially in the short wave band, where all types of environmental signals are mixed and make it challenging to detect FH signals [8]. The identification of FH signals typically occurs in two stages: parameter estimation and signal sorting [9-11]. Estimating parameters such as hop time [12], frequency [13], and angle of arrival (DOA) [14-16], is crucial for sorting multiple users without prior information in practical applications.

On the other hand, MWC structure is widely used in cognitive radar [18], estimating the direction of arrival [19], and detection of FH signals of spread spectrum systems [20], due to its features such as flexibility, sub-Nyquist sampling [17], easy implementation, etc.

In many articles, it is used to implement compressed sensing (CS) methods. However, the CS-based MWC structure has several disadvantages, such as imposing sparse condition constraints on input signals, analyzing the problem only in an underdetermined state, poor performance with reduced SNR, etc. In [21], the structure of MWC is used based on channeling and energy detection, but it is focused on a single signal without time information. In [20], MWC-based frequency analysis with dynamic programming (DP) is considered track and sort wideband FH signals in two steps. Also, the stable performance of the DP section is only for signal-to-noise ratios above 9 dB, indicating poor performance in low SNR.

FH signal analysis requires a suitable method to express time-varying signals that can simultaneously represent time and frequency variations of the signal [22]. In this regard, TF analysis is widely used to estimate FH signal parameters [3], [23-24]. In a classification for non-stationary signals, the analysis of FH signals is divided into two aspects: estimation methods based on time-frequency analysis and estimation methods without it [25]. Generally, TF analysis is divided into two parts: linear and quadratic-order analysis. Linear TF analysis mainly includes Short Time Fourier Transform (STFT), Gabor Transform, and Wavelet Transform (WD) [22]. The window used in STFT distribution is rectangular, while the window used in the Gabor transform is a Gaussian function. The rectangular function in STFT has a fixed width, so STFT has poor time-frequency resolution [26]. In addition, the time-frequency resolution of the Gabor transform is better than STFT. Also, among these transformations, wavelet transformation is one of the most effective TF analysis tools, providing a suitable approximation for signals that exhibit sharp discontinuities. However, it is a method that requires prior knowledge of a completely known signal. Generally, the main TF analysis tools [3], [27], include the STFT analysis, which has less computational complexity compared to other TF distributions. Still, its estimation error is slightly higher than other distributions [28]. The spectrogram (SPEC) distribution is considered one of the simplest quadratic-order TF analysis methods, where the time-frequency representation of the non-stationary signal energy is shown [29]. An analysis based on the Wigner-Ville distribution (WVD) provides better resolution than the SPEC distribution. Still, it introduces cross-term interference components [3]. An analysis based on the Smoothed Pseudo Wigner-Ville Distribution (SPWVD) detects cross-term in a non-cooperative environment. However, it leads to increased computational complexity and reduced performance at low SNR [24], [30-33]. An analysis based on the Re-Smoothed Pseudo Wigner-Ville Distribution (RSPWVD), which overcomes the effects of cross-term in the SPWVD distribution, and leads to increasing computational load [23]. Meanwhile, the STFT distribution analysis is linear, and the rest of the distributions are of second order. Also, in [34-35], the combined STFT-SPWVD method has been used to estimate FH signal parameters. However, the performance of this method is significantly affected by noise, and it has a high computational load [36]. Moreover, in [37] which aimed at direction finding of FH signals, a method based on relative entropy has been employed to extract a hop-free dataset, and focused on estimating the direction of arrival of the signal.

In this article, semi-blind separation of multiple asynchronous wideband FH signals using MWC and spectral entropy in the TF domain is addressed. For this purpose, in Section 2, the signal model for receiving N signals by a single antenna is investigated. In Section 3, the mathematical relationships for the proposed method, including the analysis of the MWC structure and instantaneous SE method in estimating hop times are presented. In Section 4, the results obtained from simulating the proposed method will be evaluated. Finally, in Section 5, the conclusions are presented.

2. SIGNAL MODEL

Suppose a set of N frequency-hopping signals $S = \{s_1(t), s_2(t), \dots, s_N(t)\}$, which are time-varying, asynchronous, non-stationary signals generated by fixed sources and received through a single antenna in the far field. For asynchronous FH signals, we assume the dwell time is the same. The analytical representation of the n-th received signal, at time $t \in [t_{k-1}, t_k)$ is:

$$s_n(t) = \sum_{k=1}^{N_h} \alpha_{n,k}(t) e^{j(2\pi f_{n,k}(t)t + \varphi_{n,k}(t))} \quad , \ t_{k-1} \le tk \tag{1}$$

Where $\alpha_{n,k}(t)$, $f_{n,k}(t)$ and $\varphi_{n,k}(t)$ are the amplitude, instantaneous frequency, and phase of the n-th FH signal in the k-th hop instant, respectively, and N_h is the number of frequency hops of $s_n(t)$. The k-th hop timing is defined as $t_k \in [0, T]$, and T is the observation time.

Considering linear combining model for a single antenna, the received signal $x(t)$ reads

$$x(t) = \sum_{n=1}^{N} k_n s_n(t) + n(t) \qquad ، 0 < t \leq T \quad (2)$$

Where k_n is the attenuation coefficient of the n-th signal's amplitude, and $n(t)$ is the added white Gaussian noise with zero mean and variance σ^2.

3. THE PROPOSED METHOD

In non-cooperative communications, the receiver lacks a pseudo-random sequence generator similar to the transmitter and cannot receive the frequency-hopping pattern of the signals. These receivers consist of three main parts: signal detection, parameter estimation, and separation of combined signals. Non-cooperative receivers usually receive a combination of FH signals simultaneously. Therefore, to separate the signals, the parameters of each signal are estimated [21].

We propose a semi-blind method for separating multiple asynchronous FH signals, using the MWC, TF analysis and applying an instantaneous SE-based method. The MWC structure is utilized due to its sub-Nyquist sampling [17], TF analysis is used because of its simplicity and fast computations [40] in analyzing time-varying signals [41] and also for evaluating the parameters of FH signals in blind mode [42]. Additionally, SE method is used for estimation of signal parameters such as hop times [37]. Some features of the proposed MWC_TF_SE method for the Blind Source Separation (BSS) process are as follows:

1- Signal processing capability in the baseband [38] and sub-Nyquist sampling [17], [39], employing a single antenna.
2- Analysis of MWC structure in TF domain and simultaneous extraction of time and frequency information of signals.
3- Separation of signals based on the TF_SE method.
4- Removal of other interfering signals.

In summary, the proposed method consists of two stages for solving the BSS problem:

(1) Passing signals through MWC, and transfer to the TF domain.
(2) Instantaneous SE method in the estimation of signal parameters.

In the following, the proposed method is presented in detail.

3.1. MWC structure

In the context of the BSS process using a narrow-band receiver, two flexible and popular structures of random demodulator (RD) and MWC can be mentioned. These structures can be employed in spectrum sensing to alleviate the limitations caused by the bandwidth shortage of receivers for wideband signals. In the meantime, the RD is a well-known single-branch structure for recovering the input signal, with m_0 limited frequency components, such as $\{e^{jl\omega_0}\}_{l=1}^{m_0}$. It is suitable for implementing analytical methods like CS. However, it leads to complex integral computations. Therefore, it is possible to use an alternative wideband converter, such as MWC, which is a generalization of the RD structure Some of the features of multi-branch compared to single-branch MWC are:

1. Parallel Processing and Data Diversity: Multiple branches allow parallel processing of the input signal, which can lead to the extraction of diverse features from different branches simultaneously. This can enhance the system's ability to capture various characteristics of the input signal.

2. Improved Signal Separation: In cases where the input signal contains different components or sources, multiple branches can help separate and process these components independently, potentially leading to more accurate signal decomposition.

3. Enhanced Noise Robustness: By processing the input signal through multiple branches and then combining the results, noise and interference from one branch may be mitigated by the information gathered in other branches, resulting in a more robust output.

4. Feature Combination: Having multiple branches allows for the combination of features extracted from each branch, potentially yielding more comprehensive and informative representations of the input signal.

Fig. 1 illustrates the standard structure of MWC. Consider the frequency band range $\mathcal{F} \triangleq [-f_{nyq}/2، f_{nyq}/2]$ for the signal $x(t)$, where $f_{nyq}/2$ is the upper limit of the frequency band $x(t)$.

According to the figure (1), the signal $x(t)$ is multiplied by a set of periodic sequences $p_i(t)، i \in \{1، \dots، M\}$. These periodic sequences have a period of $T_p = 1/f_p$ and a frequency range of $\mathcal{F}_p \triangleq [-f_p/2، f_p/2]$, as defined by

(3

Then, MWC passes the resulting product through the low-pass filter $h(t)$ in the frequency range $\mathcal{F}_s \triangleq [-f_s/2, f_s/2]$, and it samples the filter output uniformly at a frequency of f_s, while satisfying the conditions of $f_s \geq f_p$ ، $f_s \ll f_{nyq}/2$ [17]. In this case, the output signal of the i-th branch is equal to

$$y_i[n] = \left(\left(x(t) \times p_i(t)\right) \underset{t}{*} h(t)\right)\Big|_{t=nT_s} = \int_{-\infty}^{\infty} x(\tau) p_i(\tau) h(t-\tau) dt \Big|_{t=nT_s} \quad (4)$$

Where $x(t)$ is the input signal, $p_i(t)$ is the periodic sequence of the i-th branch, $h(t)$ is the baseband filter, $\boldsymbol{y}_i = \{y_i[0], y_i[1], \dots, y_i[\mathrm{L}_y - 1]\}$, L_y is the length of the $\boldsymbol{y}_i$, and $T_s = 1/f_s$ is the sampling time interval. Considering M branches of MWC, the set of vectors $\boldsymbol{y} = \{\boldsymbol{y}_1, \boldsymbol{y}_2, \dots, \boldsymbol{y}_{\mathrm{M}}\}$ is obtained at the output of MWC.

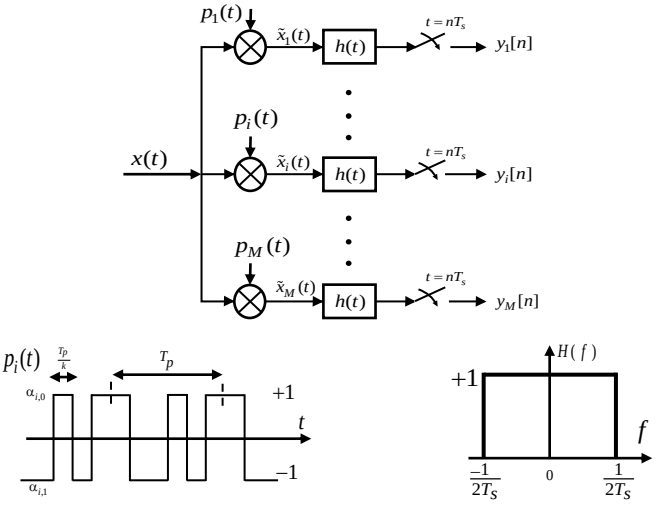

Fig1. MWC structure consisting of M parallel channels [17]

By simultaneously processing each of the signals in the set $\boldsymbol{y}$, a set of signal features will be obtained. By processing these features, the desired parameter can be extracted. But the increase in the number of MWC branches leads to an increase in the volume of calculations. Therefore, it is possible to select one of the signals of the set $\boldsymbol{y}$ and perform further processing on it. In this case, the effects of noise and interference in the selected signal are less observed compared to other members. In this article, the second mode is chosen.

3.1.1. TFD of MWC output data

TF distribution is an analytical tool that provides time and frequency information of signals simultaneously. In the BSS process using TF distribution leads to recovery and estimating signal parameters.

According to the Eq. (*a*-5) in Appendix (A), the discrete TF distribution of the observed signal at the output of the i-th MWC branch is equal to

$$\boldsymbol{\rho}_{\boldsymbol{y}_i}[n,k] = \sum_{|m| < \frac{N_G}{2}} \boldsymbol{G}[n,m] \underset{n}{*} (y_i[n+m] y_i^*[n-m]) e^{-j2\pi km/N_{\mathrm{G}}} \quad (5)$$

where y_i^* is the conjugate of y_i, $\boldsymbol{G}[n,m]$ is the time-lag kernel, and $[n,m] \in \mathbb{Z}$. By considering M branches of MWC, the set of distributions $\{\boldsymbol{\rho}_{\boldsymbol{y}_i}[n,k]\}_{i=1}^{\mathrm{M}}$ is obtained where $\boldsymbol{\rho}_{\boldsymbol{y}_i}[n,k]$ is the discrete TF distribution of the observed vector $\boldsymbol{y}_i$.

In the next stage of the signal separation process, by applying the instantaneous SE method on the distribution $\boldsymbol{\rho}_{\boldsymbol{y}_i}[n,k]$, we will take a significant step toward recovering the signals.

3.2. Spectral entropy

The spectral entropy of a signal is a measure of its spectral power distribution. The concept is based on the Shannon entropy, or information entropy. The SE treats the signal's normalized power distribution in the frequency domain as a

probability distribution, and calculates its Shannon entropy. This property is useful for feature extraction [43-44], and is also widely used in areas such as signal processing [37], and biomedical signal processing [45].

FH signal structure has a unique feature compared to other signals. When the frequency changes, a discontinuity will appear in the frequency spectrum of the signal. Methods based on entropy, variance, etc, are sensitive to discontinuous points in the signal, and can be used to extract information from these points. In this article, by applying the instantaneous SE method to the $\boldsymbol{\rho}_{y_i}[n,k]$ matrix, such as the STFT matrix, the hopping times of FH signals are determined.

3.2.1. Instantaneous spectral entropy estimation

To estimate SE, we obtain the TFD matrix in the output of one of the MWC branches, such as the SPEC distribution. According to Eq. (*a*-7) of Appendix (A), the STFT distribution for the i-th MWC branch is equal to

$$\boldsymbol{\rho}_{y_{i\_STFT}}[n,k] = \sum_{m=1}^{M_\omega} \boldsymbol{y}_i[m+n]\omega[m]e^{\frac{-j2\pi km}{M_\omega}} \qquad (6)$$

where $\boldsymbol{\omega} = \{\omega[1], \omega[2], \dots, \omega[M_\omega]\}$ is the window function, and M_ω is the number of samples of $\boldsymbol{\omega}$. In the STFT distribution, an analysis window, such as Hamming window, slides over the signal and then the Discrete Fourier Transform (DTF) is computed for the windowed data. The number of rows in the STFT matrix equals the number of DFT points, and the number of columns is given by $l = \left\lfloor \frac{L_y - L}{R} \right\rfloor$, $l \geq 2$, where L_y is the length of $\boldsymbol{y}_i$, and $R = L_\omega - L$ represents the hop distance between consecutive DFT, L_ω is the length of $\boldsymbol{\omega}$.

Each column of the STFT matrix is a spectral segment of the signal and provides a short-term estimate of the time-frequency content of the signal [43]. The STFT matrix in terms of spectral segments can be expressed as $\boldsymbol{Y}_i(f) = [Y_{i,1}(f)\ Y_{i,2}(f) \dots\ Y_{i,m}(f) \dots\ Y_{i,l}(f)]$. The element corresponding to m-th row and h-th column of the matrix $\boldsymbol{Y}_i(f)$ is equal to

$$Y_{i,m}(f_h) = \sum_{n=-\infty}^{\infty} y_i[n]\omega[n-mR]e^{-j2\pi f_h n} \qquad (7)$$

For $f_h \in \{f_1, f_2, \dots, f_{N_f}\}$, where N_f is the number of DFT points,and the vector $Y_{i,m}(f) = \left[Y_{i,m}(f_1), Y_{i,m}(f_2), \dots, Y_{i,m}\left(f_{N_f}\right)\right]^T$ is obtained [43].

The probability function for each column of the STFT matrix is used for detecting hop times. Columns, with frequency hops have high entropy due to the presence of instantaneous frequency variations. Entropy can be regarded as a measure of uncertainty between pairwise elements of a discrete set. Any possibility of displacement between the elements of this set, which have close probabilities, increases the entropy of the collection. In a time window with frequency hopping from one moment to another, it causes the signal to show its spectrum dispersion with a high entropy value.
Generally, the spectral entropy in the domain (t,f) is defined in terms of TF distributions as follows [22]:

$$\mathcal{SE} = -\sum_{n=1}^{N_t}\sum_{k=1}^{N_f} \frac{\boldsymbol{\rho}_{\mathbf{y}}[n,k]}{\sum_n \sum_k \boldsymbol{\rho}_{\mathbf{y}}[n,k]} \log_2\left(\frac{\boldsymbol{\rho}_{\mathbf{y}}[n,k]}{\sum_n \sum_k \boldsymbol{\rho}_{\mathbf{y}}[n,k]}\right) \qquad (8)$$

where N_t , N_f are the total time and frequency points, respectively. The above relation is only valid for the TFDs that do not assume negative values, e.g., the SPEC. Considering the STFT distribution, the instantaneous SE of the i-th MWC branch is equal to

$$\mathcal{SE}_{i,(t)} = -\sum_{k=1}^{N_f} \frac{\boldsymbol{\rho}_{y_i\_STFT}[n,k]}{\sum_k \boldsymbol{\rho}_{y_i\_STFT}[n,k]} \log_2\left(\frac{\boldsymbol{\rho}_{y_i\_STFT}[n,k]}{\sum_k \boldsymbol{\rho}_{y_i\_STFT}[n,k]}\right) \qquad (9)$$

where $\mathcal{SE}_{i,(t)} \in \mathbb{C}^{N_t}$. In every time window, as long as the frequency is constant, the elements of $\mathcal{SE}$ remain constant, as soon as the frequency changes, the elements of $\mathcal{SE}$ show significant change and is considered a hop time.

Therefore, by applying the SE method to the STFT matrix of the SPEC distribution, a set of peaks is created in the spectrum. In the next step, by detecting and processing these peaks, signal parameters are separated and estimated.

3.2.2. Estimating hop times of signals

In practice, the presence of frequency hop in the signal leads to an increase in the SE spectrum. Therefore, detecting peak points is essential for extracting time and frequency measurement information from the signal.

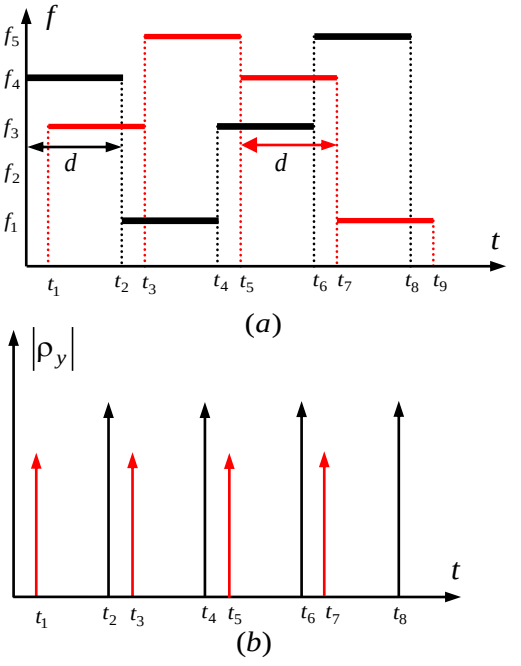

Fig. 2. (*a*) shows the sample distribution of SPEC for two asynchronous FH signals with four frequency hops, (b) the SE of Figure (*a*) in the ideal state, and the creation of impulse functions at hop times.

Fig. (*a*-2) shows the SPEC distribution of two asynchronous FH signals with four frequency hops. The frequency dwell time, d, is the same for all frequency hops in both signals. Figure (*b*-2) shows the performance of the TF_SE method in an ideal state, where a set of impulse functions is created at the time instants of signal hops.

According to Eq. (10), extraction of signal peaks based on instantaneous SE and obtain a set of frequency-hopping times $\{\hat{t}_{i,hop}\}$ of the signals.

$$\hat{t}_{i,hop} = \arg\left\{\max_{t}\left[\left|\mathcal{SE}_{i,(t)}\right|\right]\right\},\ 0 \le \hat{t}_{i,hop} \le \mathrm{NN_h} \qquad (10)$$

where $\mathrm{N_h}$ represents the number of frequency hops per signal, and N is the number of signals. Increasing SNR in the SE method leads to a reduction in false peaks and improvement in the estimating the set of time instants $\{\hat{t}_{hop}\}$. Considering that all equations are related to a single branch, in order to simplify the equations, the i variable has been omitted in the following equations.

3.3. Separation of hop times

By Applying the TF_SE method, a set of hop times, $\{\hat{t}_{hop}\}$, is obtained. In this stage, to separate the hop times of each signal, we first sort the set of times $\{\hat{t}_{hop}\}$ in ascending order. Then, by measuring the difference between each successive pair of time values $\{\hat{t}_{hop}\}$,

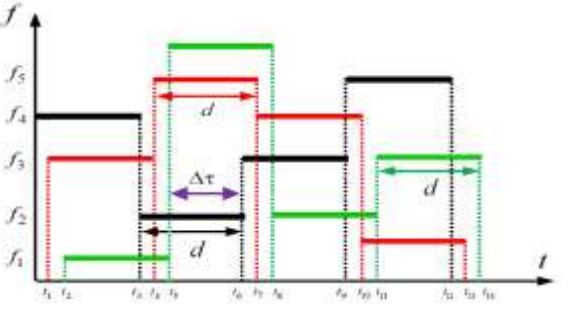

Fig. 3. The representation of three asynchronous FH signals, each with four hopping frequencies and the same dwell time.

a set of rounded numbers is obtained as follows:

$$t_{hopdif} = \{\Delta \hat{t}_{hop}\} \quad (11)$$
$$= \text{diff}\,\{t_1, t_2, t_3, t_4, t_5, t_6, t_7, \dots\}$$
$$= \{\Delta t_1, \Delta t_2, \dots, \Delta t_m, \dots, \Delta t_{\hat{k}}\}$$

where $\hat{k} = \text{NN}_\text{h} - 1$ and $\Delta t_m = t_m - t_{m-1}$ for $1 < m \leq \hat{k}$.

It is assumed that all three signals have the same dwell time as shown in Figure (3). Some of the features of the t_{hopdif} vector are as follows:

- In the t_{hopdif} set, the highest frequency (with a value of N_h) corresponds to the time delays between the signals. that is,

$$Max(\Delta \hat{t}_{hop}) = \{\Delta t_1, \Delta t_2, \Delta t_4, \Delta t_5, \Delta t_7, \Delta t_8, \dots$$
$$\dots, \Delta t_{\hat{\text{N}}_\text{h}-5}, \Delta t_{\hat{\text{N}}_\text{h}-4}, \Delta t_{\hat{\text{N}}_\text{h}-2}, \Delta t_{\hat{\text{N}}_\text{h}-1}\}$$

where $\hat{\text{N}}_\text{h} = \text{NN}_\text{h}$, $\Delta t_1 = t_1 - 0$, $\Delta t_2 = t_2 - t_1$, $\Delta t_4 = t_4 - t_3$,… and that,

$$\Delta\tau_1 = \Delta t_1 = \Delta t_4 = \Delta t_7 = \Delta t_{10} = \cdots = \Delta t_{\hat{\text{N}}_\text{h}-2}$$
$$\Delta\tau_2 = \Delta t_2 = \Delta t_5 = \Delta t_8 = \Delta t_{11} = \cdots = \Delta t_{\hat{\text{N}}_\text{h}-1}$$

where $\Delta\tau_1$ represents the delay time between the first and second signals, and $\Delta\tau_2$ represents the delay time between the second and third signals.

- In the set t_{hopdif}, after $\Delta\tau_1$, the highest frequency (with a value of $\text{N}_\text{h} - 1$) corresponds to the set $\{\Delta t_3, \Delta t_6, \Delta t_9, \dots, \Delta t_{\hat{\text{N}}_\text{h}-3}\}$, In which, $\Delta t_3 = t_3 - t_2$, … and that,

$$\Delta\tau = \Delta t_3 = \Delta t_6 = \Delta t_9 = \dots = \Delta t_{\hat{\text{N}}_\text{h}-3}$$

So, for three signals, $t_\tau = \{\Delta\tau_1, \Delta\tau_2\}$ represents the time delay between the signals, and $t_C \approx \Delta\tau + \Delta\tau_1 + \Delta\tau_2$ will dwell time d.

- In the t_{hopdif} set, the repetition of all three consecutive components indicates the accuracy of the MWC_TF_SE method, in estimating the two parameters t_τ and t_C. According to Figure (3), and Eq.(11), the equality $\Delta\tau_1 = \Delta t_m$, which means that in the m-th hop, the m-th component of all three signals is correctly estimated.
- Previous properties of the t_{hopdif} set are discussed in the ideal state, but in practice, factors such as environmental noise, and SNR reduction lead to a decrease in the frequency of $\Delta\tau_1$ and $\Delta\tau_2$.
- So, Increasing the frequencies $\Delta\tau_1$ and $\Delta\tau_2$ in the t_{hopdif} set, leads to an increase the accuracy of the TF_SE method.

Generally, for N asynchronous FH signals, assuming the dwell time is the same, the set of hop times for each signal can be recovered and separated using two parameters t_τ and t_C, as follows:

$$\text{Signal\_1}: \{0, t_C, 2t_C, \dots\}$$
$$\text{Signal\_2}: \{\Delta\tau_1, t_\text{C} + \Delta\tau_1, 2t_\text{C} + \Delta\tau_1, 3t_\text{C} + \Delta\tau_1, \dots\}$$
$$\text{Signal\_3}: \{\Delta\tau_1 + \Delta\tau_2, t_\text{C} + (\Delta\tau_1 + \Delta\tau_2), \dots \quad 2t_\text{C} + (\Delta\tau_1 + \Delta\tau_2), \dots\} \vdots$$
$$\text{Signal\_N}: \{(\Delta\tau_1 + \Delta\tau_2 + \cdots + \Delta\tau_{N-1}), \dots$$
$$t_\text{C} + (\Delta\tau_1 + \Delta\tau_2 + \cdots + \Delta\tau_{N-1}), \dots$$
$$2t_\text{C} + (\Delta\tau_1 + \Delta\tau_2 + \cdots + \Delta\tau_{N-1}), \dots\}$$

By extracting the hop times from the STFT matrix of the TF distribution, other information, such as hopping frequencies, energy density of T-F plane points, period, and frequency hop of each signal based on matrix STFT, can be determined and separated.

One of the advantages of the proposed method is that in a real environment, FH signals have time interference with other environmental signals, such as burst, constant, periodic, and other signals. However, if the two parameters t_τ and t_C are accurately estimated, the interfering signals will not impact the estimation of signal parameters, and are easily eliminated.

Because, the basis of recovery of signal hopping times is based on the difference frequency of both consecutive components of the time vector $\{\hat{t}_{hop}\}$, and disturbing signals lack frequency due to scattering. Therefore, they have little effect on the estimation process of t_τ and t_C, and can be easily removed.

Also, in the proposed method, according to the level of signal contamination with noise, the accuracy of estimating time parameters decreases, and leads to an increase in estimation error. Therefore, improving processing variables, such as increasing SNR, increasing input samples, increasing experiment repetitions, etc, results in a reduction of estimation errors for time parameters t_τ and t_C, consequently leading to increased accuracy in separating the time intervals of each signal hop.

4. EVALUATION OF THE PROPOSED METHOD

This section is intended to validate the proposed method in the article, and it aims to evaluate, and calculate errors in the estimated parameters. We consider three asynchronous FH signals, each of these signals consists of six frequency hops ($\mathrm{Nh} = 6$). The signals have different magnitudes [1.4 1.6 1.7], zero phases, different hop times, and the same hop length.

The signals are placed in the frequency band range of $50\mathrm{MHz} \le f \le 550\mathrm{MHz}$, without frequency interference. Table (1) shows the normalized frequency-hopping pattern of the three input sources.

Table 1. Frequency-hopping pattern of input signals.

Inputs	Normalized hopping frequencies
Signal (1)	$\{0.05, 0.14, 0.445, 0.28, 0.48, 0.165\}$
Signal (2)	$\{0.22, 0.51, 0.19, 0.07, 0.41, 0.225\}$
Signal (3)	$\{0.545, 0.385, 0.115, 0.32, 0.35, 0.09\}$

Figure (4) shows the SPEC distribution of asynchronous FH signal over a period. In the asynchronous mode, the hopping times of FH signals are different. According to the figure (4), the total hopping time for all signals is equal to $t_C = 2\mu$ seconds (hopping rate $f_h = 500k\mathrm{Hz}$), but the signals have time delays relative to each other. To simulate MWC input, for a sampling rate of $f_S = 600\mathrm{MHz}$, the number of sampling points is $N_S = t_C * f_S = 1200$. An increase in f_S or the duration of t_C leads to an increase in the value of N_S. Increasing the number of N_S points for each frequency- hopping leads to improved estimation of hopping parameters with less error and better accuracy. However, increasing N_S leads to increased computational complexity and hardware limitations.

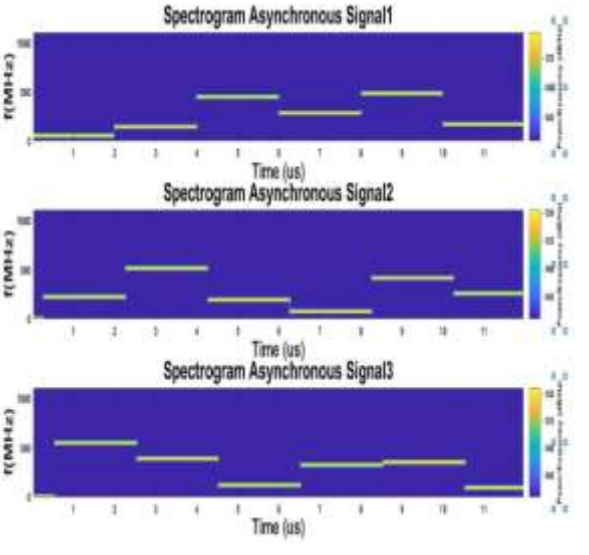

Fig. 4. SPEC, distribution of three asynchronous input signals.

Therefore, for designing a suitable system, a trade-off between variables should be considered. Table (2) shows the numerical values of MWC parameters.

Table 2. MWC parameters.

Parameter	Value	Parameter	Value
Number of branches (M)	**10**	Sampling frequency	**5MHz**
Sequence compression (k)	**30**	Filter bandwidth (B)	**2.5MHz**

According to Table (2), a low-pass filter with a limited bandwidth of 2.5MHz has been used to pass FH signals with a frequency-hopping range of 500MHz.

According to Eq. (10), Figure (5-a) shows the amplitude of $\mathcal{SE}_{(t)}$ in terms of time, to display the hop times of FH input signals. Each of these signal consists of six frequency hops. The duration of each hop for every signal is the same, and equal to $t_C = 2\mu$ seconds. According to Figure (5-a), all hopping times are equivalent to:

$$t_{hop}(\mu S) = \begin{pmatrix} 0 & 2 & 4 & 6 & 8 & 10 \\ 0.17 & 2.16 & 4.16 & 6.17 & 8.17 & 10.16 \\ 0.34 & 2.33 & 4.33 & 6.34 & 8.32 & 10.33 \end{pmatrix}$$

The signals have a time delay relative to each other of approximately $t_\tau = 0.17\mu$ seconds.

Fig. (5-b) shows the results obtained from estimating the hop times of the signals in the MWC output. The estimation error is reduced by repeating the experiment, and increasing the SNR.

As shown in Figure (5-b), in Experiment 400, for over 100 iterations, the hop times of the signals with an error less than 1.068×10^{-7}, sorted from small to large, have been estimated as follows:

$$\hat{t}_{hop}(\mu S) = \{0 \text{ ، } 0.18 \text{ ،}0.35 \text{ ،}2 \text{ ،}2.18 \text{ ،}2.35 \text{ ،}4 \text{ ،}4.18 \text{ ،}4.35 \\ \text{ ، } 6 \text{ ،}6.18 \text{ ،}6.35 \text{ ،}8 \text{ ،}8.18 \text{ ،}8.35 \text{ ،} 10 \text{ ،} 10.18 \text{ ، } 10.35\}$$

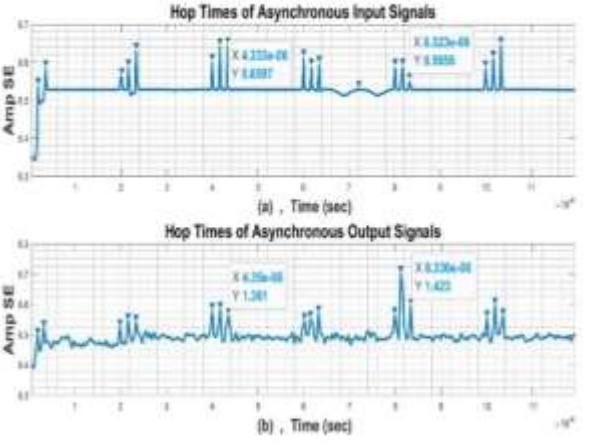

Fig. 5. (a) plotting the amplitude of $\mathcal{SE}_{(t)}$ in terms of time, and showing the hop times of three input asynchronous FH signals **(b)** Estimated hop times at MWC output.

In addition, In a noisy environment, decreasing the SNR leads to an increase in false peaks in the spectrum, and applying the SE method significantly increases the estimation error.

By measuring the difference of both consecutive components of the time vector $\hat{t}_{hop}$, A set of rounded numbers is obtained as follows:

$$t_{hopdif} = \{13.1 \text{ ،}166.4 \text{ ،}17.5 \text{ ،}17.5 \text{ ،}166.4 \text{ ،}17.5 \text{ ،}17.5 \text{ ،} 166.4 \\ 13.1 \text{ ،}17.5 \text{ ،}166.4 \text{ ،}13.1 \text{ ،}21.9 \text{ ،}166.4 \text{ ،}17.5 \text{ ،}17.5\}$$

In this set, the number 17.5 is observed with the highest frequency value, which indicates the time delay between signals. Because, it is the same frequency dwell time for all FH signals in each frequency hop. The higher the frequency value, the higher the accuracy of the SE method. Additionally, increasing the SNR leads to an increase in the frequency value.

In the next step, the position of each pair of consecutive and repeating numbers, 17.5, in the vector t_{hopdif} represents the time delay of three signals at hop times. For example, in the t_{hopdif} vector, the third and fourth components have a

common value of 17.5, indicating that in the second hop, the second component of all three signals has been correctly registered. Similarly, the sixth and seventh components of the t_{hopdif} vector have the same value. it means, The SE method has correctly estimated the third time component of all three signals in the third hop. Also, the total value of 166.4, along with two delays of 17.5, indicates the approximate duration of each signal at a constant frequency.

Therefore, using the t_{hopdif} vector, it is possible to obtain the time delay between signals (i.e., $t_\tau = 0.175 \times 10^{-6}$) , and the approximate time t_C (i.e., $t_C = 2 \times 10^{-6}$).

Considering the t_{hopdif} vector, the second, third, and sixth components of all three signals can be estimated using two-time parameters, t_τ, and t_C. For example, the third component of all three signals is equal to the following:

$$\text{Signal\_1}(3) = 10^{-6}\{2 \times t_C + 0 \times t_\tau\} = 4\mu Sec$$
$$\text{Signal\_2}(3) = 10^{-6}\{2 \times t_C + 1 \times t_\tau\} = 4.175\mu Sec$$
$$\text{Signal\_3}(3) = 10^{-6}\{2 \times t_C + 2 \times t_\tau\} = 4.35\mu Sec$$

Similarly, the sixth component of the signals is:

$$\text{Signal\_1}(6) = 10^{-6}\{5 \times t_C + 0 \times t_\tau\} = 10\mu Sec$$
$$\text{Signal\_2}(6) = 10^{-6}\{5 \times t_C + 1 \times t_\tau\} = 10.175\mu Sec$$
$$\text{Signal\_3}(6) = 10^{-6}\{5 \times t_C + 2 \times t_\tau\} = 10.35\mu Sec$$

Thus, using the estimated time parameters t_τ and t_C, the set of hop times for each signal can be recovered and separated as follows:

$$\text{Signal\_1}(\mu S): \{0 \text{ ،} 2 \text{ ،} 4 \text{ ،} 6 \text{ ،} 8 \text{ ،} 10\}$$
$$\text{Signal\_2}(\mu S): \{0 \text{ ،} 2.17 \text{ ،} 4.17 \text{ ،} 6.17 \text{ ،} 8.17 \text{ ،} 10.17\}$$
$$\text{Signal\_3}(\mu S): \{0 \text{ ،} 2.35 \text{ ،} 4.35 \text{ ،} 6.35 \text{ ،} 8.35 \text{ ،} 10.35\}$$

As previously mentioned, improving processing variables, such as increasing SNR, increasing Ns, and increasing the repetition of experiments result in reducing the estimation errors of time variables t_τ and t_C to less than 10^{-8} (and even zero). As a result, the accuracy is increased in separating the hop times of each signal.

4.1. Calculating the RMS/RF error

To evaluate the results of the analysis, the estimated hop time errors have been measured using RMSE and RFE methods. The estimation error of hop times is defined using Eq. (12) and Eq. (13).

$$RMSE_t = \sqrt{\frac{1}{NRU'}\sum_{n=1}^{N}\sum_{r=1}^{R}\sum_{u=1}^{U'}\left(t_{nr}^{(u)} - \hat{t}_{nr}^{(u)}\right)^2} \qquad (12)$$

In Eq. (12), $\hat{t}_{nr}^{(u)}$ represents the estimated hop time, $t_{nr}^{(u)}$ represents the actual value of the hop time, n indicates the n-th signal, and r for the r-th frequency of the signal hop.

$$RFE_t = \frac{1}{U'}\sum_{u=1}^{U'}\frac{|\hat{t}_{h_u} - t_h|}{f_S} \qquad (13)$$

In Eq. (13), $\hat{t}_{h_u}$ represents the estimated time, t_h represents the actual value of the hop time, f_S for the sampling frequency of the MWC, and U′, represents the total number of experiments. It should be noted that for all calculations, the number of experiments is greater than $U' = 400$. Naturally, increasing U′ leads to improvements in the results.

Figure (6), displays the curve of the RMS error value compared to the RF error for estimating hop times of three asynchronous FH signals at different SNR values. The results are obtained by registering the error for $8 \times 20 = 160$ processing iterations.

According to the Figure (6), the RMS error has decreased compared to the RF error and recorded a smaller amount of error, so that in the value of SNR $= -1dB$, the RMS error is approximately 0.25 of the RF error and recorded a value of 0.54×10^{-6}. In addition, in low and negative SNR values, the RMS error is more reduced. Also, in the value of SNR $= 3dB$, the RMS error amount has almost reached zero, and in this case, the hopping times are estimated with better accuracy. It should be noted that the amount of recorded error has a direct relationship with the amount of rounding of the estimated hopping times during processing.

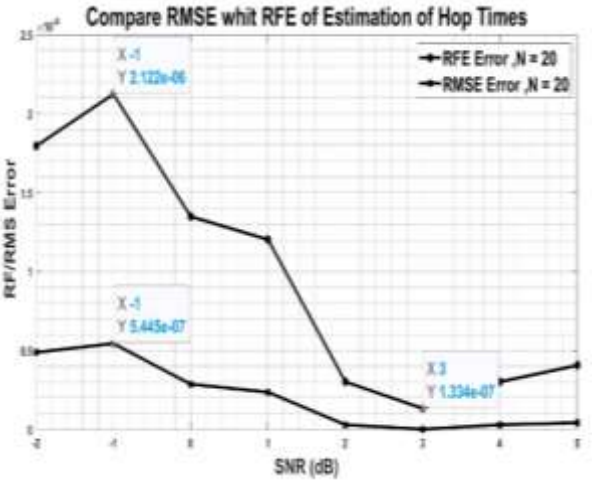

Fig 6. Compares, the RF error value with RMS in estimating the hopping times of three asynchronous FH signals.

Figure (7), shows the curve of the RMS error value compared to the RF error for estimating the hopping times of three asynchronous FH signals. The repetition of processing is $8 \times 200 = 1600$. According to the figure(7), increasing the repetition by 10 times has led to an error reduction of approximately 0.1 while maintaining the previous features compared to figure (6).

In another investigation, the increase in the number of experiments and its impact on the RMS error for three signals with six hop frequencies has been examined. As shown in Figure (8), increasing n results in a reduction in the RMS error of the system. Moreover, at low SNR values, the error slope becomes slow and nearly linear.

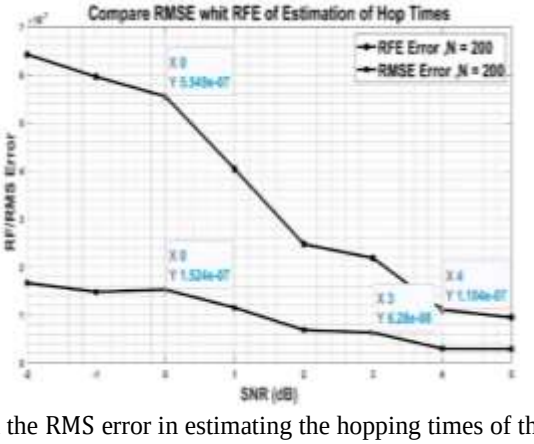

Fig. 7. Compares, the RF error with the RMS error in estimating the hopping times of three asynchronous FH signals with increased processing repetition.

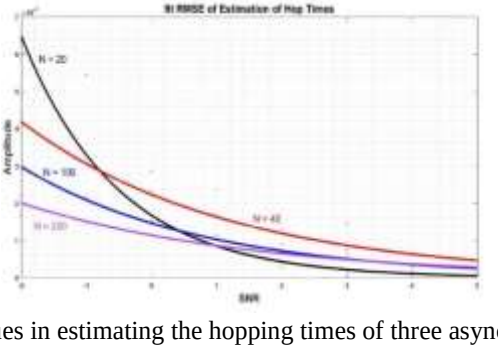

Fig. 8. Shows, the RMS error values in estimating the hopping times of three asynchronous HF signals for different numbers of processing repetitions.

4.2. Comparison with other methods

In this section, to validate the accuracy of the proposed method compared to other methods, the estimation accuracy of parameters has been evaluated in terms of SNR for three asynchronous signals. Figure (9), For $Nh = 6$, compares the RMS error curve of the MWC_TF_SE method within the range of SNR -4dB to 10dB, simultaneously with two other methods, the STF distribution based on array processing [8], and the parameter estimation method using sparse linear regression (SLR) [46]. The results represent the recorded error rate for a processing repetition of $15 \times 100 = 1500$ times.

According to the figure (9), the proposed method has achieved better results than the $STFD-$ based method using ULA over the entire SNR range. Moreover, for $SNR \leq +1.5dB$, the RMS error of the proposed method is significantly reduced. So, in $SNR = -4dB$, the recorded error is approximately half of the other two techniques.

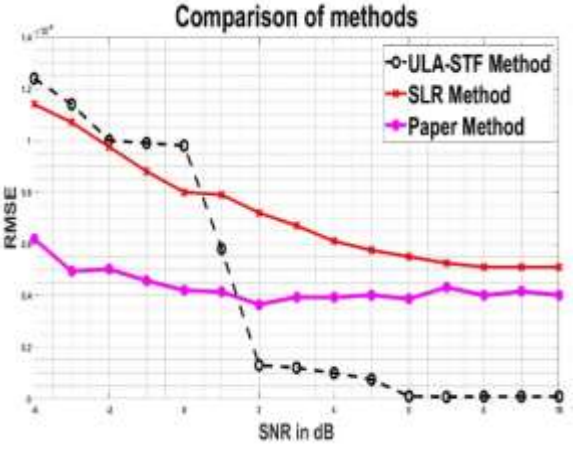

Fig. 9. Compares, the RMS error of different methods in estimating the hopping times of FH signals.

Additionally, in the entire SNR range, the slope of the error curve for the proposed method is slow, indicating its robustness compared to the other two techniques. However, for $SNR > 7dB$, the error of the research method converges towards a constant value of 0.4×10^{-6}. This is due to the rounding errors in the parameter extraction process of the signal. Another point to note is that increasing variables, such as the number of sampling points, SNR, and the number of iterations significantly contribute to improving results and reducing errors.

5. CONCLUSION

This paper proposes a novel Semi-BSS and parameters estimation method of FH signals. The proposed method exploits the structure of MWC and SE method to estimating the parameters of FH signals. In the proposed method, initially, three FH signals in the frequency range of $50 \leq f(\text{MHz}) \leq 550$ were received by a single antenna and passed through MWC.

The MWC structure consists of ten branches with a constant sampling rate of $f_s = 5\text{MHz}$, and a receiver with a cut-off frequency of $f_{cut} = 2.5\text{MHz}$. Then, the instantaneous SE method was applied to the TF distribution of the output data from MWC. The accurate estimation of the time delay variables, t_τ, and the duration of stay, t_C, ensures the precision of the proposed method in signal separation and parameter estimation. Some features of the proposed MWC_TF_SE method for the BSS process are as follows:

- Signal processing capability in the baseband and sub-Nyquist sampling condition by a single antenna,
- Ability to remove interfering arrival of the signals,
- Improved performance of the method with reduced SNR, compared to similar methods for $SNR \leq +1.5dB$ values,
- Significant reduction in the volume of data in the input TF analysis, proportional to the MWC sampling rate, and increased program execution speed.

The obtained evaluation results show that this algorithm has an acceptable performance compared to other traditional separation methods, is applicable at lower SNR, and has higher accuracy. According to Figure (9), the error rate decreases significantly compared to other methods at $SNR \leq +1.5dB$. Specifically, around $SNR = -4dB$, the RMS error reaches an approximate value of 0.6×10^{-6}, representing a 50% reduction compared to other methods in parameter estimation.

REFERENCES

[1] Yun-Bin، Y. and T. Qing-Min ، "**DOA Estimation Methods of FH Signals and Follower Gamming Signals**"، J. Nav. Univ. Eng 28، pp. 228-234، 2016.

[2] R. L. Peterson، D. E. Borth، and R. E. Ziemer، "**An Introduction to Spread-Spectrum Communications**"، Prentice-Hall، Inc، 1995.

[3] S. Barbarossa and A. Scaglione، "**Parameter Estimation of Spread Spectrum Frequency-Hopping Signals Using Time-Frequency Distributions**، " in Signal Processing Advances in Wireless Communications، First IEEE Signal Processing Workshop on، Paris، France، pp. 213-216، 1997.

[4] H. Alizadeh, M. Rezaee and M. Babaei, "**Amplitude Symmetry Detection for Interfering Signals in CNC Satellite Communications**"، Majlesi Journal of Telecommunication Devices (MJTD), Volume 12, Issue3, Pages 149-159, September 2023.

[5] Y. Yuan، Z. Huang، and X. Wang، ``**Detection of frequency-hopping radio frequency-switch transients،'' Electron. Lett.**، vol. 50، pp. 956_957، Jun. 2014.

[6] J. Viterbi، "**Spread spectrum communications: myths and realities**،" IEEE Communications Magazine، vol. 40، no. 5، pp.34–41، 2002.

[7] X. Liu، N. D. Sidiropoulos، and A. Swami، "**Joint hop timing and frequency estimation for collision resolution in FH networks**،" IEEE Transactions onWireless Communications، vol. 4، no. 6، pp. 3063–3073، 2005.

[8] J. Wan، D. Zhang، W. Xu، and Q. Guo، " **Parameter Estimation of Multi-Frequency Hopping Signals Based on Space-Time-Frequency Distribution**"، Symmetry، Vol. 11، No.5، pp.648، 2019.

[9] L. Wan، X. Kong، and F. Xia، "**Joint Range-Doppler-Angle Estimation for Intelligent Tracking of Moving Aerial Targets**،" IEEE Internet of Things Journal، vol. 5، pp. 1625-1636، 2018.

[10] S. Tomar and P. Sumathi، "**Amplitude and Frequency Estimation of Exponentially Decaying Sinusoids**،" IEEE Transactions on Instrumentation and Measurement، vol.67، pp.229-237، 2018.

[11] L. Wan، G. Han، L. Shu، S. Chan، and T. Zhu، "**The Application of DOA Estimation Approach in Patient Tracking Systems with High Patient Density**،" IEEE Transactions on Industrial Informatics، vol. 12، pp. 2353-2364، 2016.

[12] D. Angelosante، G. B. Giannakis، and N. D. Sidiropoulos، "**Estimating Multiple Frequency-Hopping Signal Parameters via Sparse Linear Regression**،" IEEE Transactions on Signal Processing،vol.58، pp. 5044-5056، Oct 2010.

[13] Z. C. Sha، Z. T. Huang، Y. Y. Zhou، and F. H. Wang، "**Frequency-hopping signals sorting based on underdetermined blind source separation**،" Iet Communications، vol. 7، pp. 1456-1464، 2013.

[14] L. Wan، G. Han، L. Shu، S. Chan، and N. Feng، "**PD Source Diagnosis and Localization in Industrial High-Voltage Insulation System via Multimodal Joint Sparse Representation**،" IEEE Transactions on Industrial Electronics، vol. 63، pp. 2506-2516، 2016.

[15] L. Wan، G. Han، L. Shu، and N. Feng، "**The Critical Patients Localization Algorithm Using Sparse Representation for Mixed Signals in Emergency Healthcare System**"، IEEE Systems Journal، vol. 12، pp. 52-63، 2018

[16] L. Wan، G. Han، L. Shu، N. Feng، C. Zhu، and J. Lloret، "**Distributed Parameter Estimation for Mobile Wireless Sensor Network Based on Cloud Computing in Battlefield Surveillance System**"، IEEE Access، vol. 3، pp. 1729-1739، 2015.

[17] M. Mishali، and Y. C. Eldar، "**From Theory to Practice: Sub-Nyquist Sampling of Sparse Wideband Analog Signals**"، IEEE Journal of Selected Topics in Signal Processing، Vol. 4، No. 2، pp. 375-391، 2010.

[18] E. Baransky، G. Itzhak، N. Wagner، I. Shmuel، E. Shoshan، and Y. Eldar، " **Sub-Nyquist Radar Prototype: Hardware and Algorithm**"، IEEE Transactions on Aerospace and Electronic Systems، Vol. 50، NO. 2، pp. 809-822، 2014.

[19] S. S. Ioushua، O. Yair، D. Cohen، and Y. C. Eldar، "**CaSCADE: Compressed Carrier and DOA Estimation**"، IEEE Transactions on Signal Processing، Vol. 65، No.10، pp. 2645-2658، 2017.

[20] Z. Lei، Y. Peng، Z. Linhua، X. Hui، and D. Hong، "**Frequency Hopping Signals Tracking and Sorting Based on Dynamic Programming Modulated Wideband Converters**"، Applied Sciences، Vol. 9، No. 14، pp. 2906، 2019.

[21] Z. Lei، P. Yang، and L. Zheng، "**Detection and Frequency Estimation of Frequency Hopping Spread Spectrum Signals Based on Channelized Modulated Wideb and Converters**"، Electronics، Vol. 7، No.9، pp. 170، 2018.

[22] B. Boashash، "**Time-Frequency Signal Analysis and Processing: A Comprehensive Review**"، 2nd ed.: Elsevier Science، eBook، 2015.

[23] Y. Lei and Y. Wu، "**A New Hop Rate Estimation Method for High-Speed Frequency-Hopping Signals**"، in 2008 11th IEEE Singapore International Conference on Communication Systems، Guangzhou، China، pp.1330-1333، 2008.

[24] T. C. Chen، "**Joint Signal Parameter Estimation of Frequency-Hopping Communications**"، Iet Communications، vol. 6، pp. 381-389، Mar 2012.

[25] Y. Wang، Y. Lin، & X. Chi، "**A Parameter Estimation Method of Frequency Hopping Signal Based on Sparse Time-Frequency Method**"، In 2018 IEEE 23rd International Conference on Digital Signal Processing (DSP)، pp. 1-5، November 2018.

[26] R.G. Stockwell، L. Mansinha، R.P. Lowe، "**Localization of the complex spectrum: the S transform**"، IEEE Trans. Signal Process، vol. 44، no. 4، pp. 998-1001، 1996.

[27] W. Yang، M. Li، & L. Wang، H. Zhang، "**Parameter Estimation of Frequency Hopping Signals Based on Time Frequency Analysis**"، In Proceedings of the 26th conference of spacecraft TT\&C technology in China، pp. 131–140، 2013.

[28] Q. Zhang، Y. Liu، X. Zhang، "**Parameter Estimation of Non_modulated or Modulated Frequency-Hopping Signals**"، IEEE International Conference on Signal Processing، Communications and Computing. IEEE، pp. 1-4، 2016.

[29] L. Deng، T. Zhang، J. Jin، "**Application of Rearrangement Spectrogram in Parameter Estimation of Frequency-Hopping Signal**"، Computer Engineering and Design، Vol. 34، No. 10، pp. 3422–3426، 2013.
[30] T. Jo Lynn، "**Adaptive Optimal Kernel Smooth-Windowed Wigner-Ville Distribution for Digital Communication Signal**، EURASIP Journal on Advances in Signal Processing، 2009.
[31] Liang، Z.-J.; Lv، M، " **A joint rapid parameter estimate method of frequency-hopping signals**"، In Proceedings of the 2012 International Conference on Control Engineering and Communication Technology، Shenyang، Liaoning، China، 7–9 December، pp. 952–954، 2012.
[32] Zhang، H.-X.; Chen، C.-F.; Wang، H.-Q، "**A parameter estimation method for FH signal based on SPWVD**"، J. China Univ. Posts Telecommun، 18، pp. 133–136، 2011.
[33] Y. Yang، X. Sun، and Z. Zhong، "**A Parameter Estimation Algorithm for Frequency-Hopping Signals with a Stable Noise**"، C IEEE 3rd Advanced Information Technology، Electronic and Automation Control Conference (IAEAC)، pp. 1898-1904، 2018.
[34] W. H. Fu، Y. Q. Hei، and X. H. Li، "**UBSS and blind parameters estimation algorithms for synchronous orthogonal FH signals**"، Journal of Systems Engineering and Electronics، vol. 25، no. 6، pp. 911–920، 2014.
[35] W. H. Fu، W. Lu، K. Jia، et al، "**Blind Parameter Estimation Algorithm for Frequency Hopping Signals Based on STFT and SPWVD**"، Journal of Huazhong University of Science and Technology، vol. 42، no. 9، pp. 59–63، 2014.
[36] Y. Li، X. Guo، F. Yu، and Q. Sun، "**A New Parameter Estimation Method for Frequency Hopping Signals**"، IEEE USNC-URSI Radio Science Meeting، (Joint with AP-S Symposium)، pp. 51-52، 2018.
[37] M. Khazaee، and S. Akhlaghi، "**Direction-of-Arrival and Hop Tracking of A Special User in A FH Multi-User Based Network Using Uniformly Linear Arrays**"، Journal of Ra'ad،Vol. 5، No. 12، pp. 10-26، 2016. (In Persian)
[38] J. P. Changeux، and S. J. Edelstein، " **Allosteric mechanisms of signal transduction**"، Science، Vol. 308، No. 5727، pp. 1424-1428، 2005.
[39] M. Mishali، Y. C. Eldar، D. Oleg، and Sh. Eli، "**Xampling: Analog to digital at Sub-Nyquist Rates**"، IET Circuits، Devices & Systems Vol. 5، No. 1، pp. 8-20، 2011.
[40] Yang، W.-G.، Li، M.، & Wang، L.-B.، et al ، "**Parameter estimation of frequency hopping signals based on time frequency analysis**"، In Proceedings of the 26th conference of spacecraft TT\&C technology in China، pp. 131–140، 2013
[41] Guido، R.C.; Addison، P.S.; Walker، J، "**Introducing Wavelets and Time-Frequency Analysis Wavelet-Related Technologies in Biomedical Signal Processing**"، IEEE Eng. Med. Biol، vol. 28، no. 13، 2009.
[42] Feng، T.; Yuan، C.-W، "**Blind parameter estimation of frequency-hopping signals based on the time–frequency distribution maxima**"، Acta Electron، vol. 39، pp. 2921–2925، 2012
[43] Pan، Y. N.، J. Chen، and X. L. Li، "**Spectral Entropy: A Complementary Index for Rolling Element Bearing Performance Degradation Assessment**"، Proceedings of the Institution of Mechanical Engineers، Part C: Journal of Mechanical Engineering Science. Vol. 223، pp. 1223–1231، 2009.
[44] Sharma، V.، and A. Parey، "**A Review of Gear Fault Diagnosis Using Various Condition Indicators**"، Procedia Engineering. Vol. 144، pp. 253–263، 2016.
[45] Vakkuri، A.، A. Yli-Hankala، P. Talja، S. Mustola، H. Tolvanen-Laakso، T. Sampson، and H. Viertiö-Oja، "**Time-Frequency Balanced Spectral Entropy as a Measure of Anesthetic Drug Effect in Central Nervous System during Sevoflurane، Propofol، and Thiopental Anesthesia**"، Acta Anaesthesiologica Scandinavica. Vol. 48، pp. 145–153، 2004.
[46] L. Zhao، L. Wang، G. Bi، L. Zhang، and H. Zhang، "**Robust Frequency-Hopping Spectrum Estimation Based on Sparse Bayesian Method**"، IEEE Transactions on Wireless Communications، Vol. 14، No. 2، pp. 781-793، 2014.
[47] Civera, Marco, and Cecilia Surace، **"Instantaneous spectral entropy: An application for the online monitoring of multi-storey frame structures"**، Buildings, Vol.12, No. 3، pp, 310, 2022.

Appendix (A)

For the analytical signal $y[n]$, the discrete-time instantaneous autocorrelation function (IAF) is expressed by [22]:

$$\boldsymbol{K_y}[n،m] = y[n+m]y^*[n-m] \qquad (a\text{-}1)$$

where $\boldsymbol{y} = \{y[0]، y[1]، \dots، y[\mathrm{L}_y - 1]\}$, L_y is the length of $\boldsymbol{y}$, $[n،m] \in \mathbb{Z}$, and y^* is the conjugate of y. Also, the smoothed IAF (SIAF) of signal $\boldsymbol{y}$ is equal to

$$\boldsymbol{R_y}[n،m] = \boldsymbol{G}[n،m] \underset{n}{*} \boldsymbol{K_y}[n،m] \qquad (a\text{-}2)$$

where $\boldsymbol{G}[n،m]$ is the time-lag kernel, and $\underset{n}{*}$ represents the sign of discrete time-convolution. In this case, the discrete time TF distribution of the signal $\boldsymbol{y}$ is expressed by

$$\boldsymbol{\rho_y}[n،k] = \underset{m\to k}{\mathcal{DFT}}\{\boldsymbol{R_y}[n،m]\} \qquad (a\text{-}3)$$

where $[n،k] \in \mathbb{Z}$, and $\mathcal{DFT}$ represents the discrete-time Fourier transform of variable m in matrix $\boldsymbol{R_y}[n،m]$.

Substituting Eq. (*a*-2) into Eq. (*a*-3), writing out the transform, and substituting from Eq. (*a*-1), the distribution time frequency $\boldsymbol{\rho_y}[n\text{،}k]$ is obtained.

$$\boldsymbol{\rho_y}[n\text{،}k] = \sum_{|m| < \frac{N_G}{2}} \boldsymbol{G}[n\text{،}m] \underset{n}{*} (y[n+m]y^*[n-m])e^{-j2\pi km/N_G} \qquad (a\text{-}4)$$

which can be expanded as

$$\boldsymbol{\rho_y}[n\text{،}k] = \sum_{|m|<\frac{N_G}{2}} \sum_{|p|<\frac{P}{2}} \boldsymbol{G}[n-p\text{،}m]y[p+m]y^*[p-m]e^{-j2\pi km/N_G} \qquad (a\text{-}5)$$

In Eq. (*a*-4) and Eq. (*a*-5), P and N_G are a positive integer, $\boldsymbol{G}[n\text{،}m]$ is the time-lag, and $\boldsymbol{G} \in \mathbb{C}^{P\times N_G}$ [22]. For example, the time-lag kernel of some common distributions is equal to

- WV distribution
  $\boldsymbol{G}[n\text{،}m] = \delta[n]$
- SPEC distribution
  $\boldsymbol{G}[n\text{،}m] = w[n+m]w[n-m]$

WV and SPEC distributions are bilinear transformations. By placing the time-lag kernel $\boldsymbol{G}[n\text{،}m]$ of the SPEC distribution in the equation (*a*-5), the frequency-time distribution $\boldsymbol{\rho_y}[n\text{،}k]$ of the signal y[n] can be calculated.

The squared magnitude of the STFT, is called the spectrogram and is expressed as follows [22]:

$$\boldsymbol{\rho}_{\boldsymbol{y}-SPEC}[n\text{،}k] = \left|\boldsymbol{\rho}_{\boldsymbol{y}-STFT}[n\text{،}k]\right|^2 = \left|\sum_{|m|<\frac{M}{2}} y[m+n]w[m]e^{\frac{-j2\pi km}{M}}\right| \qquad (a\text{-}6)$$

2

where w[m] is the window, $\boldsymbol{\omega} = \{\omega[1]\text{،}\ \omega[2]\text{،}\ \ldots\text{،}\omega[M]\}$ $\boldsymbol{\omega}$ is of length M. According to the Eq. (*a*-6), the TF distribution of the discrete STFT is equal to

$$\boldsymbol{\rho}_{\boldsymbol{y}-STFT}[n\text{،}k] = \sum_{|m|<\frac{M}{2}} y[m+n]w[m]e^{\frac{-j2\pi km}{M}} \qquad (a-7)$$